Journal of Achievements in Materials and Manufacturing Engineering
VOLUME 32
ISSUE 2
February
2009

Effect of heat treatment on tensile and fracture toughness properties of 6082 alloy

G. Mrówka-Nowotnik*, J. Sieniawski, A. Nowotnik
Department of Materials Science, Rzeszow University of Technology,
ul. W. Pola 2, 35-959 Rzeszów, Poland
* Corresponding author: E-mail address: mrowka@prz.edu.pl

Received 15.02.2007; published in revised form 01.02.2009

Materials

ABSTRACT

Purpose: The present study investigates the effect of heat treatment parameters (temperature and time) on the tensile properties and fracture toughness of 6082 aluminium alloy.
Design/methodology/approach: Tensile strength - Rm, yield strength - Rp0.2 and elongation - A of the 6082 aluminium alloy were determined by uniaxial tensile test at room temperature. Furthermore, the aged alloy was tested in tension in order to evaluate its fracture toughness. Therefore, according to ASTM standard tests were performed on fatigue precracked compact tension (KIc) and sharp-notched specimens ( ) in both the longitudinal and transverse orientation with respect to the rolling direction.
Findings: The results show that the microstructure, mechanical properties and fracture toughness changes during artificial aging due to the precipitation strengthening process.
Practical implications: This paper is the part of previous authors' investigations which results in modification of the heat treatment parameters that may lead to the most favorable mechanical properties and fracture toughness of 6082 alloy.
Originality/value: Paper contains a broad spectrum of experimental data including uniaxial tensile test and fracture toughness investigation based on two various technique and as well as a new ideas concerning aging parameters and their effect on the mechanical properties and ductility of the 6082 alloy.
Keywords: Metallic alloys; Fracture mechanics; Mechanical properties; Heat treatment

Reference to this paper should be given in the following way:
G. Mrówka-Nowotnik, J. Sieniawski, A. Nowotnik, Effect of heat treatment on tensile and fracture toughness properties of 6082 alloy, Journal of Achievements in Materials and Manufacturing Engineering 32/2 (2009) 162-170.

1. Introduction

The 6xxx aluminium alloys have found application in automotive structures, as they offer an attractive combination of strength, formability and corrosion resistance, surface properties and good weldability. Since there is ever-increasing demand for high strength, low-cost materials, investigation of processing-microstructure relationships is strongly required. Heat treatable 6xxx aluminium alloys are of special interest for they offer hardening possibilities that lead to specific properties. It is well known that in aluminium alloys improvement of the mechanical properties is classically obtained by the precipitation produced by decomposition of the supersaturated solid solution during ageing.

© Copyright by International OCSCO World Press. All rights reserved. 2009

The hardening effects result from dislocation interaction with the precipitates acting as obstacles to the dislocation motion. Since volume fraction, chemical composition and morphology of intermetallic phases exert significant effect on the practical properties of 6xxx type Al alloys, it is also important to know where, when and what kind of intermetallic may form during solidification process [5, 9, 10, 16, 18]. Hence, the improvement of the metallurgical process and the use of heat treatable aluminium alloys as structural materials are then strongly linked to the understanding of the influence of precipitation process and intermetallics with their physical and mechanical properties on the microscopic behavior of the Al alloys.

Iron is the most common impurity in Al alloys [14]. When iron is introduced to molten aluminium in quantites above the level of 0.052%wt., it reacts with aluminum and Si to form a large number of phases during solidification process, such as Al-Fe, Al-Fe-Si and Al-Fe-Mn-Si [6, 13]. Type of these phases depends mainly on the cooling rate and the Fe/Si ratio in the alloy [4, 12]. Manganese is a common addition in 6XXX alloys. Mn increases the alloy strength as a finely precipitated intermetallics, corrects the shape of plate-like iron phases and decrease their embrittling effect. Mn combines with Fe, Si and Al exert to form α–$Al_x(Fe,Mn)_ySi_z$ phase that act as a nucleation sites for Mg_2Si particles.

The precipitation sequence for 6XXX alloys, which is generally accepted in the literature [1, 3, 8] is: SSSS →atomic clusters →GP zones →β"→ β'→ β (stable) [22]. The most effective hardening phase for this types of materials is β".

In this paper differential scanning and transmission electron microscopy (SEM, TEM) have been utilized to study the effect of the precipitation hardening on the microstructure of aluminium alloy 6082. The mechanical (R_m and $R_{p0.2}$) and plastic (A) properties of the examined alloy were evaluated by uniaxial tensile test at room temperature.

In spite of the improvements which come from advances in the processing of aluminum alloys their high strength is firmly entrenched as the material of construction up to service temperatures as high as 150°C. Further increases in reliability and efficiency of aluminum alloys require increases in strength and toughness. Hence, fracture toughness is a key property for a number of Al alloys utilized in aerospace and process industries. The most frequently used test methods for plane-strain fracture toughness of metallic materials are tests described in ASTM-standards - E399 and E602-78T [20,21]. Fracture toughness properties of the heat treated 6082 alloy were determined by performing tensile test in the presence of sharp notch R_m^k as well as compact tension test (K_{Ic} measurement technique) using samples with various orientations to the rolling direction.

2. Material and experimental

2.1. Material

The present study was carried out on 6082 aluminum alloy, containing Fe, Si, Mn and Mg as the principal elements (Table 1).

The conditions of production of the alloy were as follows: an ingot was first heated up to temperature 500°C and subsequently subjected to the extrusion forging process to obtain profiles with cross-section of a 40x100mm. The temperature of profile goes out of the press was about 550°C, the cooling on exit side of the press was not applied.

Table 1.
Chemical composition of tested 6082 Al alloy (wt%).

Element						
Si	Mg	Mn	Fe	Cr	Cu	Zn
1.2	0.78	0.50	0.33	0.14	0.08	0.05

Al - balance

2.2. Thermal processing

The thermal processing of 6082 alloy was started by a heat treatment at the temperature of uniform α solid solution. Thus the all specimens were heated in a resistance furnace for 4 hours at 575°C and quenched at room temperature. Subsequently the specimens were subjected to artificial aging at four different temperatures: 130°C for 72 h, 160°C for 50 h, 190°C for 42 h and at 220°C for 48 h.

2.3. Mechanical properties

After artificial aging, a set of specimens were prepared for tensile testing to study the effect of T6 heat treatments on mechanical properties of the examined alloys. The specimens were strained by tensile deformation on an Instron TTF-1115 servohydraulic universal tester at a constant rate, in according to standard PN-EN 10002-1:2004 [22] at room temperature. Tensile properties (tensile and yield strength; elongation) were evaluated using round test specimens of 8 mm diameter and 65 mm gauge length (according to ASTM E602-78T [20] standard – see Fig. 1a).The hardness was measured with Brinell tester under 49.03 N load for 10 sec.

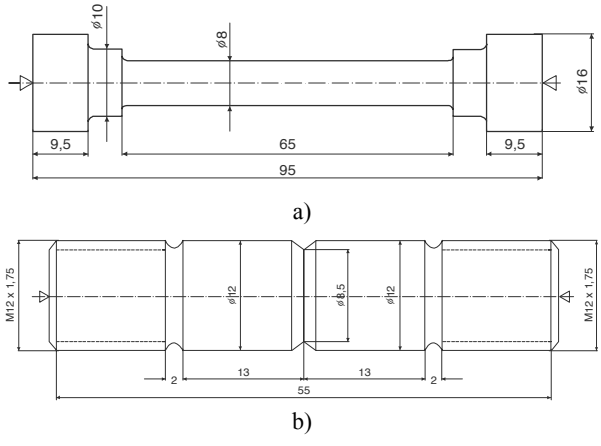

Fig. 1. Dimensions of: a) plain tensile specimens and b) sharp notched tensile specimens

In addition, sharp notched tensile and fatigue precracked compact tension specimens C(T) were machined for tension and fracture tests.

To evaluate tensile strength in the presence of a sharp notch R_m^k standard-sized specimens (12 mm diameter x 55 mm long – see Fig. 1b) containing a sharp notch (1.75 mm deep with a 8.5 mm radius) to localize the stress were used. The tensile specimens were machined such that the gauge lengths were in the transverse and longitudinal direction with respect to the rolling direction. These round tensile specimens were machined to dimensions and tolerances required by ASTM E602-78T [20].

Fatigue precracked compact tension specimens were cut from the 6082 alloys plates in longitudinal transverse L-T and transverse longitudinal T-L orientation with respect to the rolling direction. The specimen locations are illustrated in Fig. 2. Following the standard [19], the nomenclature defines applied loading axis by the first letter (L-longitudinal, T-transverse) and the direction of crack advance by the second letter.

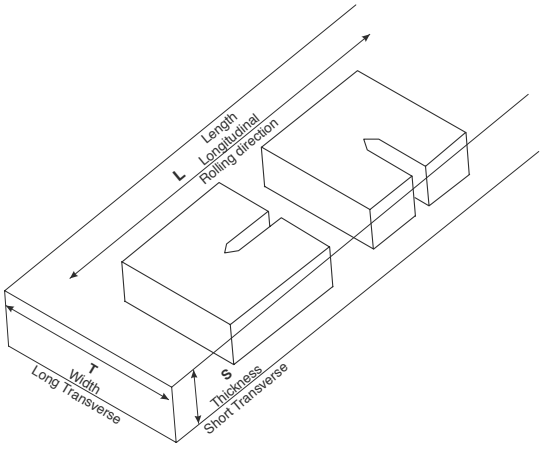

Fig. 2. Location of the compact tension specimens

The specimen dimensions and testing procedure to determine the fracture toughness K_{Ic} (critical stress intensity factor) are in accordance with the following standards: ASTM E399-85 [20], ANSI/ASTM B645-78 [19] and PN-87/H-04335 [23] (Fig. 3).

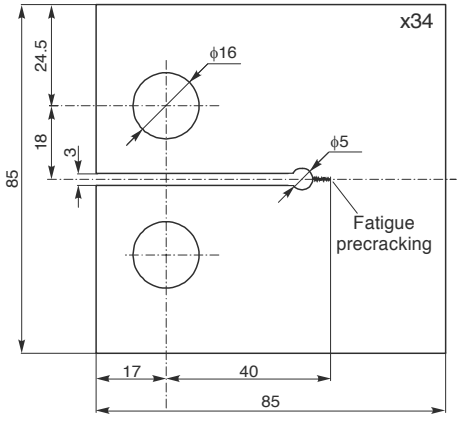

Fig. 3. Dimensions of a compact tension specimen C(T) used for fracture toughness testing - K_{Ic}

The fracture toughness was calculated using the following equation:

$$K_Q = \left(\frac{P_Q}{BW^{1/2}}\right) f\left(\frac{a}{W}\right) \quad (1)$$

where:

$$f\left(\frac{a}{W}\right) = \frac{(2+\alpha)(0{,}886 + 4{,}64\alpha - 13{,}32\alpha^2 + 14{,}72\alpha^3 - 5{,}6\alpha^4)}{(1-\alpha)^{3/2}} \quad (2)$$

where: $\alpha = \frac{a}{W}$

- B - sample thickness, mm
- W - sample width, mm
- A - crack length, mm
- K_Q - calculated crack toughness value of a material under plane-strain conditions, MPa·m$^{1/2}$
- P_Q - force, N

Experimental data were used for evaluation of crack toughness in a plane strain state - K_Q. K_Q is equal to the plane-strain fracture toughness K_{Ic} if the following criteria are satisfied:

$$a \geq 2{,}5\left(\frac{K_Q}{R_{p0,2}}\right)^2 \text{ or } B \geq 2{,}5\left(\frac{K_Q}{R_{p0,2}}\right)^2 \quad (3)$$

2.4. Metallographic investigations

Microstructure of characteristic states of examined alloy was observed using an optical microscope - Nikon 300 on polished sections etched in Keller solution (0.5 % HF in 50ml H_2O). Thin foils for TEM studies were manufactured by cutting 3 mm diameter discs, followed by grinding manually to a thickness of about 0.1 mm. Finally, the disc was thinned electrolytically using a Struers Tenupol jet polishing machine, with a solution (by volume) CH_3OH (84cm^3), HClO4 (3.5cm^3) and glycerin (12.5cm^3), operating at -10°C and U=28V. The thin foils were examined in a Tesla BS-540 and JEOL - JEM 2010 ARP TEM/STEM operated at 200kV electron microscope. Post-failure observation of the fracture surfaces of the failed C(T) specimens were made in the scanning electron microscope (SEM), operating at 6-10 kV in a conventional back-scattered electron mode

3. Results and discussion

The microstructure of the studied alloys in as-cast state is given in Fig. 4a. In the interdendritic spaces of α-Al solid solution one can see the precipitates of the intermetallic phases. The revealed particles of the intermetallic phases were formed during casting of the alloy. The typical as-cast structure of examined alloys consisted of a mixture of β-AlFeSi and α-AlFeMnSi intermetallic phases distributed at cell boundaries, connected sometimes with coarse Mg_2Si.

The microstructure of the alloy after hot extrusion forging process is given in Fig. 4b. During hot working of ingots, particles of intermetallic phases arrange in positions parallel to direction of plastic deformation (along plastic flow direction of processed material) which allows for the formation of the band structure. As a result, the reduction of size of larger particles may takes place.

The strength (R_m and $R_{p0.2}$) and plastic (A) properties of 6082 alloy after solutionizing and artificial aging at various temperatures were determined from static tensile test. The results of these tests are presented in summary Table 2.

It can be observed that as the aging time increases, a continuous increase in tensile strength, with approximately no elongation changes is noticed. An intensive hardening increment of the alloy in a relatively short time of aging not exceeded the value of 10 h, followed by further almost uniform increase in the mechanical properties within the range of longer aging times can be observed. The initial increase in the tensile strength and yield strength is due to vacancies assisted diffusion mechanism and formation of high volume fraction of (GP) zones followed by formation of metastable β'' and β' precipitates, which disturbs the regularity in the lattices (Fig. 6).

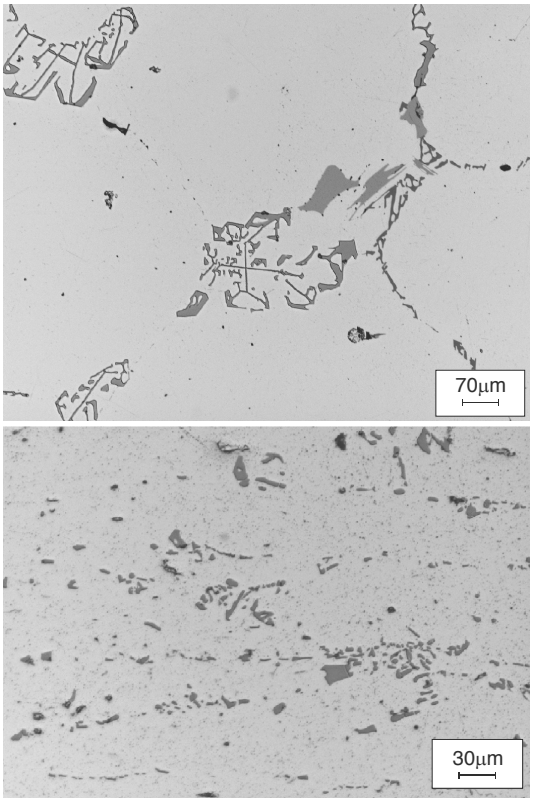

Fig. 4. Microstructure of examined 6082 alloy: a) as-cast, b) after hot extrusion

Changes in mechanical properties of the alloy treated at aging temperature of 190°C are shown in Fig. 7. These results show that tensile properties of the 6082 alloy aged at higher temperature – 190°C were almost the same as those of the alloy after aging at 130°C, and the trend of both yield strength and tensile strength variation due to aging time did not change (Fig. 7a). Thus, short aging time leads to dramatic increase of R_m and $R_{p0.2}$ values. Strength of the alloy continues to increase up to 6 hours of aging, after which there is no increase in mechanical properties, and even slightly decrease of yield strength of the alloy was observed (Fig. 7a). However, a simultaneous deterioration of plastic properties with the increase in yield strength, along with elongation of aging time, was observed. The reason for this is the same as in the case of aging at lower temperature mentioned above. Comparing these results to previous obtained for the alloy heat treated at lower temperature one can notice that the highest values of R_m and $R_{p0.2}$ were achieved within the shorter time of aging of the alloy at 190°C.

Table 2.
Mechanical properties of 6082 alloy after T6 heat treatment (solutionizing temperature 575°C)

Aging temperature, °C	Aging time, h	Mechanical properties			
		$R_{p0.2}$, MPa	R_m, MPa	A, %	Z, %
130	4	245	376	20	28.9
	10	286	402	19	26.8
	20	313	411	18	23.8
	70	350	422	18	27.2
160	2,5	250	380	20	28
	6	320	418	19	27.5
	20	362	431	18	25
	50	380	440	16,5	23.3
190	1,5	273	381	20	32.3
	2,5	323	410	18	33.5
	6	390	441	17.4	38
	30	383	418	13.4	42
220	1	385	397	13.5	40.3
	5	351	368	12.3	43.7
	30	255	297	14.5	52.6

Relatively high values of correlation coefficient (see equation in Fig. 5b) provide evidence that mechanical properties strongly depend on aging time at this temperatures.

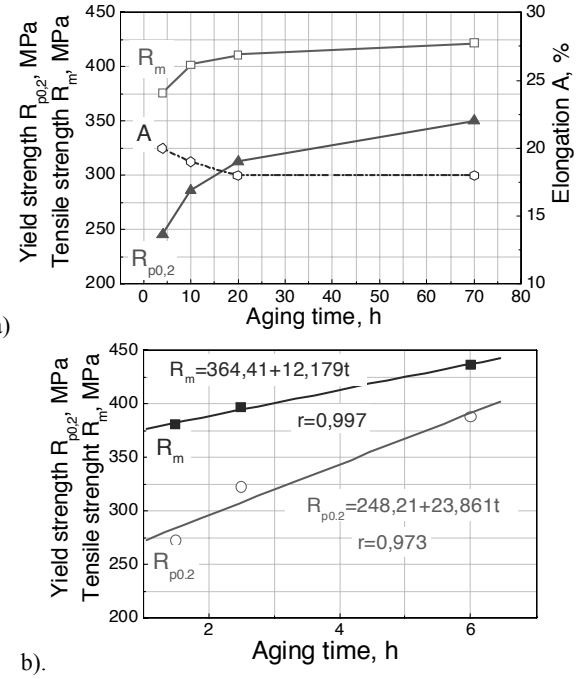

Fig. 5. Effect of time on tensile and yield strength of 6082 Al-alloy aged at 130°C

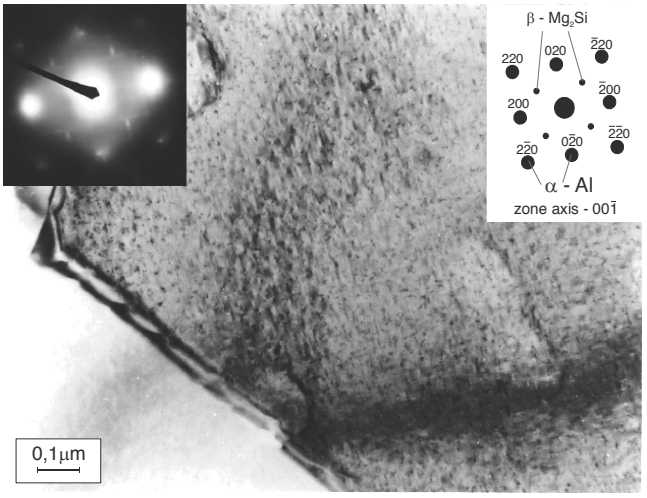

Fig. 6. TEM micrograph of 6082 alloy aged at 160°C for 6 h showing uniform dispersion of fine needle shaped of hardening β'' particles

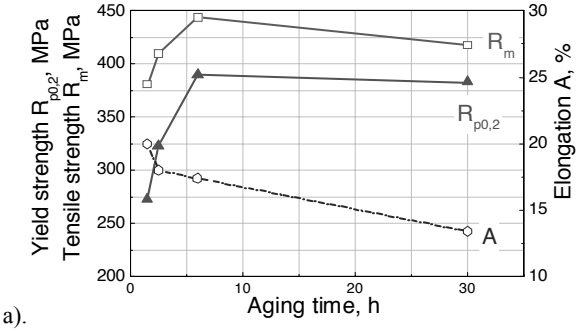

a).

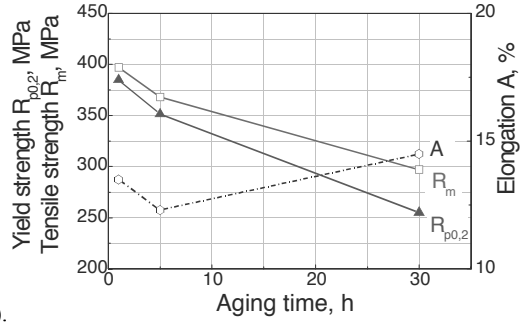

b).

Fig. 7. Effect of time on tensile and yield strength of 6082 alloy aged at: a) 190 and b) 220°C

Fig. 7b represents the curves obtained in the tensile static tests for the alloy artificially aged at the highest temperature of 220°C. There can be noted roughly linear drop of both yield strength and tensile strength with aging time. For example, the yield strength decreases significantly from its maximum 395 MPa to a value of less than 300 MPa after 30 h of aging. The maximum $R_{p0.2}$ value was recorded after 1 h of aging. However, the plastic properties increases with increasing time. Initially a minimal deterioration of elongation value was observed but at higher aging time up 5 hours the elongation values increase steadily.

Table 3 shows the variation in tensile strength in the presence of sharp notch (R_m^k) with various cleavage plane orientation to the rolling direction for the exposed alloy to aging at different temperatures and times. It was observed that the sample cut from the alloy (aged at 190°C for 5 h) in longitudinal transverse (T-L) orientation to the direction of maximum plastic deformation had the highest R_m^k value of ~ 585 MPa, as compared to that with the same cleavage plane orientation (T-L) but aged at lower temperature of 130°C and for the longest time – 70 h, which had value of ~ 505 MPa. The high tensile strength in the presence of sharp notch of the alloy exposed for 5 h at 190°C is attributed mainly to the precipitation hardening derived from the intermediate partially coherent Mg_2S hardening precipitates. Prolongation of the aging time affects in reduction of R_m^k due to growth of Mg_2S precipitates what provokes the loss of coherence with the matrix and softening of the alloy (overaging of the alloy). This produce lower tensile strength (Table 3 and Fig. 8).

Table 3.
Tensile strength in the presence of a sharp notch R_m^k of 6082 alloy

Aging temperature, °C	Aging time, h	Cleavage plane orientation	R_m^k, MPa
130	70	T-L	505
		L-T	542
190	5	T-L	553
		L-T	585
220	1	T-L	538
		L-T	575

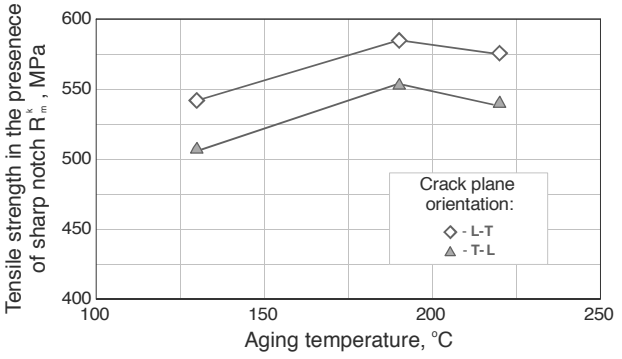

Fig. 8. The effect of aging time on tensile strength in the presence of sharp notch R_m^k of 6082 alloy

Critical stress intensity factor K_{IC} was determined using standard tensile test for 30 samples of 6082 alloy subjected to the precipitation hardening process. The crack displacement vs. load relationship, is a curve that actually represents the results of tensile test performed on the fatigue precracked samples.

The ASM has standardized 10 types of curves of varying shapes. Adequate type of a curve provide valuable data on crack growth resistance of material under static loading. According to

ASM standard the shape of the curve from Fig. 9 corresponds to type I [19,23]. Depending upon the crack plane orientation to the rolling direction, the fracture surface appears as a plane – A type, as in Fig 10a (T-L orientation) or as C type for L-T orientation, as in Fig. 10b.

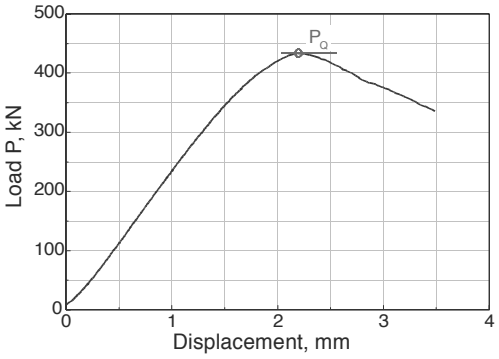

Fig. 9. Crack displacement vs. load of the sample 6082 alloy

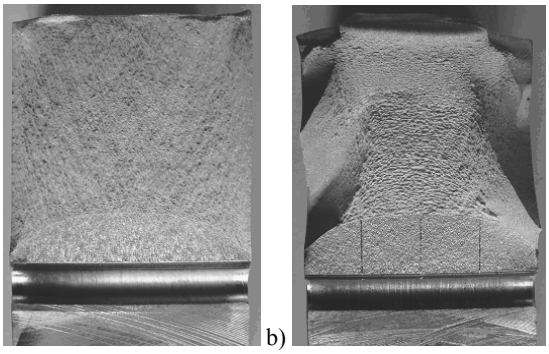

a) b)

Fig. 10. Typical fracture surface of the samples of 6082 alloy: a) T-L orientation – type A, b) L-T orientation – type C

Fracture toughness is a property which describes the ability of a material containing crack to resist fracture. Since fracture toughness is one of the most important properties of any material for all design application, it is essential for Al alloy intended for automotive structure to know if this parameters is likely to change with heat treatment conditions. The results of fracture toughness tests of the 6082 alloy are showed in Table 3. As can be seen from the listed data, toughness measurements of the specimens treated at different times and temperatures of aging and with different fracture plane orientation showed quite good agreement to the results of tensile test in the presence of sharp notch. At both test temperatures, the orientation of the crack does appear to have some influence on the toughness of the 6082 alloy. This is most likely due to the dissimilarity between the longitudinal and transverse microstructures in each heat treatment condition, Fig. 10. Samples with L-T crack orientation (perpendicular to the direction of greatest plastic deformation), regardless of aging time and temperature, had the best fracture toughness values (K_{Ic}) and were all between 36 and 43 MPa·m$^{1/2}$ (Table 4). This lead to the conclusion that the value of both $R_{p0.2}$ and K_{Ic} changes in relation to the plane orientation to the plane orientation, which means these parameters are anisotropic.

Table 4.
Average values of K_{Ic} of examined 6082 alloys (K_Q= K_{Ic})

Aging process	Fracture plane orientation	K_{Ic} MPa·m$^{1/2}$
130°C/17 h	L-T	41,0
130°C/70 h	T-L	33,1
	L-T	38,52
160°C/10 h	L-T	40,5
190°C/4,5 h	T-L	37,0
	L-T	43,34
190°C/6 h	L-T	34,5
220°C/1 h	T-L	34,0
	L-T	38,5
220°C/4,5 h	L-T	36,3
220°C/10 h	L-T	38,0
220°C/17 h	L-T	36,0

The change in yield strength with aging time for the all but one of the aged samples (excluding the alloy aged at 220°C) were identicall – $R_{p0.2}$ value increases with aging time. The yield strength of the alloy aged at 220°C going down gradually to a nearly initial values characteristic for those samples heat treated for short time at lower temperature (Fig. 11 and Table 5).

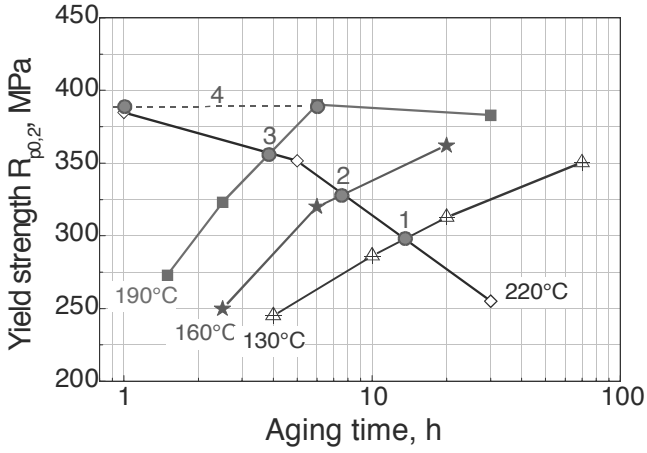

Fig. 11. The effect of the temperature and aging time on yield stress of 6082 alloy

Table 5.
The effect of the temperature and aging time on the mechanical properties of 6082 and 6005 alloy

Points in the Fig. 11 and 12	Aging process	Mechanical properties	
		$R_{p0.2}$, MPa	K_{Ic} MPa·m$^{1/2}$
1	130 °C/17h	298	41.0
	220 °C/17h		36.0
2	160 °C/10h	327	40.5
	220 °C/10h		38.0
3	190 °C/4,5h	357	37.0
	220 °C/4,5h		36.0
4	220 °C/1h	380	34.5
	190 °C/6h		34.0

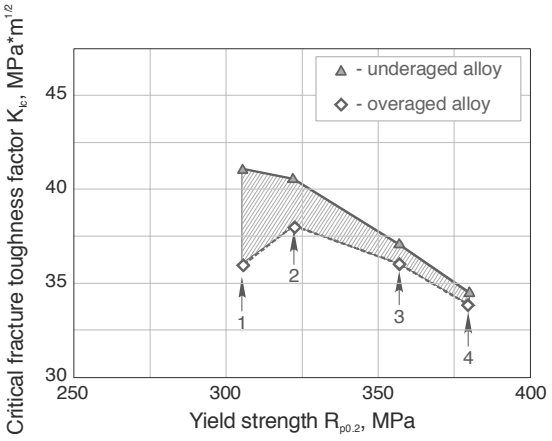

Fig. 12. The influence of yield strength $R_{p0.2}$ on the critical stress intensity factor K_{Ic} of the examined alloy – 6082

The variation in critical fracture toughness factor K_{Ic} with strength is shown in Fig. 12. The alloy heat treated at 130°C and 160°C exhibited better crack resistance to the alloy subjected to aging at higher temperature of 220°C (Fig. 12, pts: 1, 2; Table 5), which is attributed to the presence of the hardening intermetallic phases. Further, it can also be seen from Fig. 12 that the variation in K_{Ic} in the 6082 alloy with aging at 220°C for 1 h and 190°C for 6 h are almost similar (point 4), whereas $R_{p0.2}$ exhibited much larger variation with aging time at 130°C and 190°C. This is attributed to the different extents of effects of various intermetallic precipitates. Maximum decrease in $R_{p0.2}$ (Table 5) after 17 h aging at 220°C resulted from the growth of both β and α intermetallic phases – overaging process (Fig. 13) (Biroli, 2006; Warmuzek et al., 2005). Application of longer times of aging (10 and 17 h) at 130 and 160°C results in maximum value of K_{Ic} (Table 5, Fig. 12- points 1,2,3,5,).

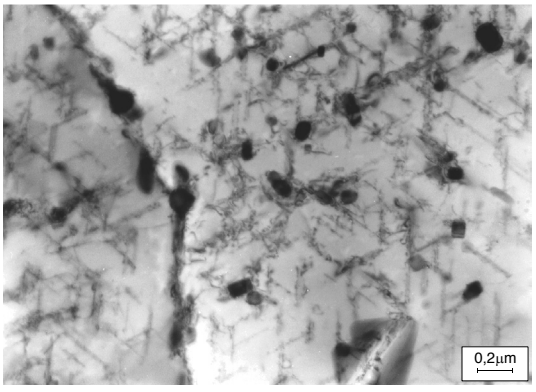

Fig. 13. Overaging alloy (300°C/20h) - pinning dislocation by large needle-like particles of β and α(Al-Fe-Mn-Si) phase.

Fractografic examination has been carried out on the fractures of the samples after a) static tensile tests (Fig. 16); b) crack resistance tests and c) tensile test in the presence of sharp notch R_m^k (Fig. 15).

Observation of the microstructure and surfaces of the failed C(T) samples showed that the fracture is facilitated by participation of few overlapping processes – nucleation, growth and coalescence of voids (Figs. 13 and 14). Most of the cracks initiated at void clusters [7,11,17].

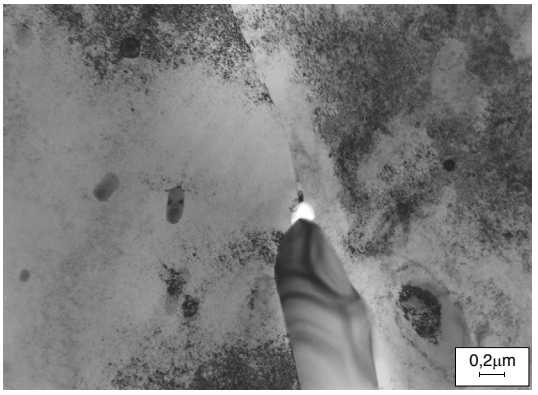

Fig. 14. TEM micrograph of the 6082 alloy subjected to the precipitation hardening process, exhibiting large iron particle

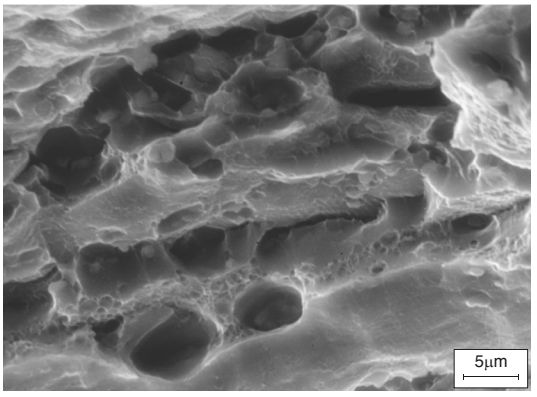

Fig. 15. Fracture surface of 6082 alloy after static notch-tensile test: a) shear oval dimples formed after coalescence of the linear void sequence b) large dimples around hard intermetallic α(Al_8Fe_2Si) and β(Al_5FeSi) precipitates and smaller around dispersive hardening β-Mg_2Si and α-Al(FeMn)Si precipitates

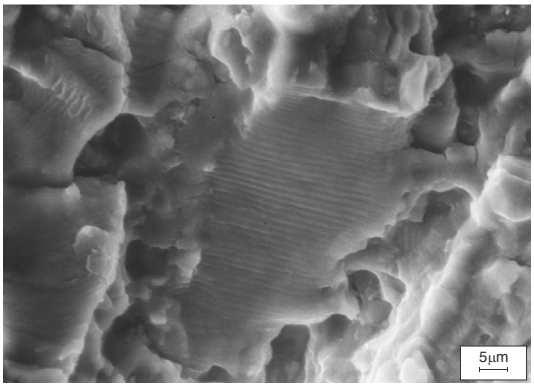

Fig. 16. Morphology of the fracture surface in the deformed 6082 alloy. Typical traces of fatigue cracking are shown

4. Conclusions

- Strength properties of artificially aged 6082 alloy are primarily affected by intermetallic precipitates - GP zones and then formation of metastable phases - β'' and β' in particular. These precipitates effectively interfere with the motion of dislocations. A decrease in the hardness and mechanical properties of the alloy in the over-aged conditions (increase in aging time and temperature) has occurred because of coalescence of the precipitates into larger particles of metastable β'' and β' phases.
- The precipitation of fine needle-shaped particles in the alloy treated at 190°C for 6 h, leads to the best mechanical properties with combination of good fracture toughness.
- Fracture toughness of 6082 alloy essentially depends on temperature and aging time as well as orientation of cleavage surface to the rolling direction. The highest value of notch-tensile strength R_m^k =585 MPa and critical stress intensity factor K_{Ic}=43,34 MPa·m$^{1/2}$ were achieved for the specimens machined in the L-T orientation and aged at 190°C for 6 hours. Similarly heat treated specimens but with T-L orientation showed following values of: R_m^k =553 MPa and K_{Ic}=37 MPa·m$^{1/2}$.
- Microstructural and fractographic examinations of tested Al alloy confirmed that cracks initiated at void clusters and were facilitated by their growth and coalescence. The sites of heterogenic nucleation of voids are the precipitates of intermetallic phases. Subsequent decohesion process initially proceeded at the interface between matrix and particle. The analysis of results revealed that 6082 alloy treated at lower temperature (130 and 160°C) for 10 i 17 h is underaged what results in higher value of K_{Ic}. Prolongation of aging time at higher temperature 220°C cause overaging of the alloy – lower K_{Ic} value.

Acknowledgements

This work was carried out with the financial support of the Ministry of Science and Information Society Technologies under grant No. 3T08B 078 27 and U-6572/BW.

References

[1] G. Biroli, G. Caglioti, L. Martini, G. Riontino, Precipitation kinetics of AA4032 and AA6082 a comparison based on DSC and TEM, Scripta Materialia 39/2 (1998) 197-203.
[2] Y. Biroli, The effect of processing and Mn content on the T5 and T6 properties of AA6082 profiles, Journal of Materials Processing Technology 173 (2006) 84-91.
[3] G.A. Edwards, K. Stiller, G.L. Dunlop, M.J. Couper, The precipitation sequence in Al-Mg-Si alloys, Acta Materialia 46/11 (1998) 3893-3904.
[4] A.K. Gupta, D.J. Lloyd, S.A. Court, Precipitation hardening in Al-Mg-Si alloys with and without excess Si, Materials Science and Engineering A316 (2001) 11-17.
[5] S. Karabay, M. Zeren, M. Yilmaz, Investigation of extrusion ratio effect on mechanical behaviour of extruded alloy AA-6101 from the billets homogenised-rapid quenched and as-cast conditions, Journal of Materials Processing Technology 160 (2004) 138-147.
[6] N.C.W. Kuijpers, W.H. Kool, P.T.G. Koenis, K.E. Nilsen, I. Todd, S. Van der Zwaag, Assessment of different techniques for quantification of α-Al(FeMn)Si and β-AlFeSi intermetallics in AA 6xxx alloys, Materials Characterization 49 (2003) 409-420.
[7] Z. Li, A.M. Samuel, C. Rayindran, S. Valtierra, H.W. Doty, Parameters controlling the performance of AA319-type alloys: Part II. Impact properties and fractography, Materials Science and Engineering A367 (2004) 111-122.
[8] W.F. Miao, D.E. Laughlin, Precipitation hardening in aluminum alloy 6022, Scripta Materialia 40/7 (1999) 873-878.
[9] G. Mrówka-Nowotnik, J. Sieniawski, Influence of heat treatment on the microstructure and mechanical properties of 6005 and 6082 aluminium alloys, Proceedings of the 13th International Scientific Conference "Achievements in Mechanical and Materials Engineering" AMME'2005, Gliwice−Wisła, 2005, 447-450.
[10] G. Mrówka-Nowotnik, J. Sieniawski, Influence of heat treatment on the micrustructure and mechanical properties of 6005 and 6082 aluminium alloys, Journal of Materials Processing Technology 162-163 (2005) 367-372.
[11] G. Mrówka-Nowotnik, J. Sieniawski, A. Nowotnik, Tensile properties and fracture toughness of heat treated 6082 alloy, Journal of Achievements in Materials and Manufacturing Engineering 17 (2006) 105-108.
[12] G. Sha, K. O'Reilly, B. Cantor, J. Worth, R. Hamerton, Growth related phase selection in a 6xxx series wrought Al alloy, Materials Science and Engineering A304-306 (2001) 612-616.
[13] R.A. Siddiqui, H.A. Abdullah, K.R. Al.-Belushi, Influence of aging parameters on the mechanical properties of 6063 aluminium alloy, Journal of Materials Processing Technology 102 (2000) 234-240.
[14] M. Warmuzek, G. Mrówka-Nowotnik, J. Sieniawski, Influence of the heat treatment on the precipitation of the intermetallic phases in commercial AlMn1FeSi alloy, Journal of Materials Processing Technology 157-158 (2004) 624-632.
[15] M. Warmuzek, K. Rabczak, J. Sieniawski, The course of the peritectic transformation in the Al-rich Al–Fe–Mn–Si alloys,

Journal of Materials Processing Technology 162-163 (2005) 422-428.
[16] M. Warmuzek, J. Sieniawski, A. Gazda, G. Mrówka, Analysis of phase formation in AlFeMnSi alloy with variable content of Fe and Mn transition elements, Materials Engineering 137 (2003) 821-824.
[17] M. Wierzbińska, J. Sieniawski, Effect of morfology of eutectic silicon crystals on mechanical properties and cleavage fracture toughness of AlSi5Cu1 alloy, Journal of Achievements in Materials and Manufacturing Engineering 14 (2006) 31-36.
[18] S. Zajac, B. Bengtsson, Ch. Jönsson, Influence of cooling after homogenization and reheating to extrusion on extrudability and final properties of AA 6063 and AA 6082 alloys, Materials Science Forum 396-402 (2002) 675-680.
[19] ANSI/ASTM B645-78. Standard Practice for plane-strain fracture toughness testing of aluminium alloys.
[20] ASTM E399-85. Standard method of test for plane-strain fracture toughness of metallic materials.
[21] ASTM E602-78T. Tentative method for Sharp-notch tension testing with cylindral specimens.
[22] PN-EN 10002-1+AC1. Metals. Standard method of tensile test at room temperature.
[23] PN-87/H-04335. Standard method for plane-strain fracture toughness.